Electronic Supplementary Material (ESI) for Journal of Materials Chemistry A.

Supporting Information

An In-Situ and General Preparation Strategy for Hybrid Metal/Semiconductor Nanostructures with Enhanced Solar Energy Utilization Efficiency

Hua Bai,[a] Fang Ye,[a] Qing Lv,[a] Guangcheng Xi,*[a] Junfang Li,[a] Haifeng Yang,[a] and Chongqing Wan*[b]

[a] Nanomaterials and Nanoproducts Research Center, Chinese Academy of Inspection and Quarantine, No. 11, Ronghua Sough Roude, Beijing, 100176, China.
[b] Department of Chemistry, Capital Normal University, No. 105, North Road, West 3th Ring Road, Beijing, 100048.

Xiguangcheng@caiq.gov.cn
wancq@cnu.edu.cn

Experimental Section

Synthesis of Metal/MoO_3 Hybrid Nanobelts: In a typical synthesis, 0.35 g of H_2MoO_4 and 4mL of concentrated hydrochloric acid (37%) was added into 100 ml of distilled water, and a white suspension was formed immediately. The white suspension was then loaded into a Teflon-lined autoclave. The autoclave was sealed, heated in an oven of 180 °C for 20 h, and then naturally cooled to room temperature, and a blue flocculent product (MoO_{3-x}) formed, which was then collected, washed with ethanol and distilled water several times to remove ions and possible remnants. 0.5 g of the as-synthesized MoO_{3-x} was added into 100 ml distilled water under mild stir. The aqueous solution of noble metal precursors (H_2PtCl_6, H_2AuCl_5, $AgNO_3$, and $PdCl_2$) was dropped into the MoO_{3-x} suspension. After 24 h stirring, the final product was collected, washed with ethanol and water, and dried in air. For example, in a typical synthesis of Ag loaded MoO_3 (6.3 %, 4 nm) hybrid composite, 6 mL of $AgNO_3$ (0.01 g/mL) aqueous solution was dropped into the MoO_3 suspension under strong stirring. The dropping rate is about 0.5 mL per minute. The colour of the mixture charged quickly from blue to dark gray. After 24 h stirring, the final product was collected, washed with ethanol and distilled water several times, and dried in air at 60 °C for 6 h.

Photocatalytic Degradation Dyes: The photocatalytic activities of the hybrid nanobelts were evaluated by degradation of azo dyes (rhodamine B, methyl orange, and methylene blue) in an aqueous solution under visible light from a 300W Xe lamp (71PX300 LX–300; 7–s Technology) equipped with cutoff filter L42 and a water filter. The visible light intensity is about 27 mW cm^{-2}. The photocatalyst (0.1 g) was poured into 100mL dye solution (10 mg/L) in a Pyrex reactor at room temperature under air. Before light was turned on, the solution was continuously stirred for 30 min in dark to ensure the establishment of an adsorption–desorption equilibrium. The concentration of dye during the degradation was monitored by colorimetry using a UV-vis spectrometer (Shimadzu UV-3600).

Photocatalytic Synthesis of Benzyl compounds: The photocatalytic activities of the hybrid nanobelts were further evaluated by preparation of benzalaniline ($C_{13}H_{11}N$) from toluene and aniline under visible light ($\lambda \geq 420$ nm) irradiation from a 300W Xe lamp (HSX-F300, NBeT). The photocatalyst (50 mg) was poured into 20 mL toluene solution (contains 50 □l of aniline) in a sealed quartz reactor at room temperature.

Before light was turned on, the suspension was continuously stirred for 30 min in dark to ensure the establishment of an adsorption–desorption equilibrium. The concentration of benzalaniline and aniline during the photocatalytic process was monitored by colorimetry using a gas chromatography-mass spectrometry (Agilent 6890/5975 GC-MS, USA).

Characterization: XRD patterns of the products were recorded on a Rigaku D/max–γA X–ray diffractometer by using CuKα radiation (λ = 1.54178 Å). Scanning electron microscopy (SEM) images were obtained on a JEOL–6700F. Transmission electron microscopy (TEM) and high–resolution TEM (HRTEM) characterizations were performed with a JEOL 2100 operated at 200 kV. BET measurements were carried out in Micromeritics Tristar 3000. UV–Vis-NIR absorption spectra were recorded with a Shimadzu UV-3600. Fourier transform infrared (FTIR) spectra were obtained from THERMO Iz10.

Synthesis of Metal/Semiconductor Hybrid materials by Traditional Method: For the preparation of supported Au colloidal materials, an aqueous solution of $HAuCl_4$ of the desired concentration were prepared. Fresh solutions of poly (vinyl alcohol) (PVA) (1 wt% aqueous solution, Aldrich, MW=10 000, 80% hydrolyzed) and an aqueous solution of $NaBH_4$ (0.1 M) were also prepared. For example, a catalyst comprising Au nanoparticles with 5 wt% total metal loading on a MoO_3 nanobelt support was prepared as follows: To an aqueous $HAuCl_4$ solution of the desired concentration, the required amount of a PVA solution (1 wt %) was added (PVA/Au (w/w) = 1.2); a freshly prepared solution of $NaBH_4$ (0.1 M, $NaBH_4$/Au (mol/mol = 5) was then added to form a dark-brown sol. After 30 min of sol generation, the colloid was immobilized by adding MoO_{3-x} nanobelts under vigorous stirring conditions. The amount of support material required was calculated to have a total final metal loading of 5.6 wt%. After 2 h, the slurry was filtered and the catalyst was washed thoroughly with distilled water and dried at 60°C overnight. The catalysts were treated at 400 °C under static air for 3h using a heating rate 2 °C.

Synthesis of V_2O_{5-x} Nanowires: In a typical synthesis, 0.4 g of V_2O_5, 2 mL of concentrated hydrochloric acid (37%), and 10 mL of ethanol were added into 80 ml of distilled water. The mixture was then loaded into a Teflon-lined autoclave. The autoclave was sealed, heated in an oven of 160 °C for 18 h, and then naturally cooled to room temperature, and a black-blue product formed, which was then collected, washed with ethanol and distilled water several times to remove ions and possible remnants.

Synthesis of TiO_{2-x} Nanoplates: The synthetic method is referenced to the report of Prof. Christopher B. Murray et al. In a modified 40 mmol of oleylamine, 8 mL of 1-octadecene, and 0.5 mL of oleic acid, 50 mL of ethanol, and 0.5g of TiF_4 are mixed and then added into a Teflon-lined autoclave. The autoclave was sealed, heated in an oven of 220 °C for 20 h, and then naturally cooled to room temperature, and a blue product formed, which was then collected, washed with ethanol and distilled water several times to remove ions and possible remnants.

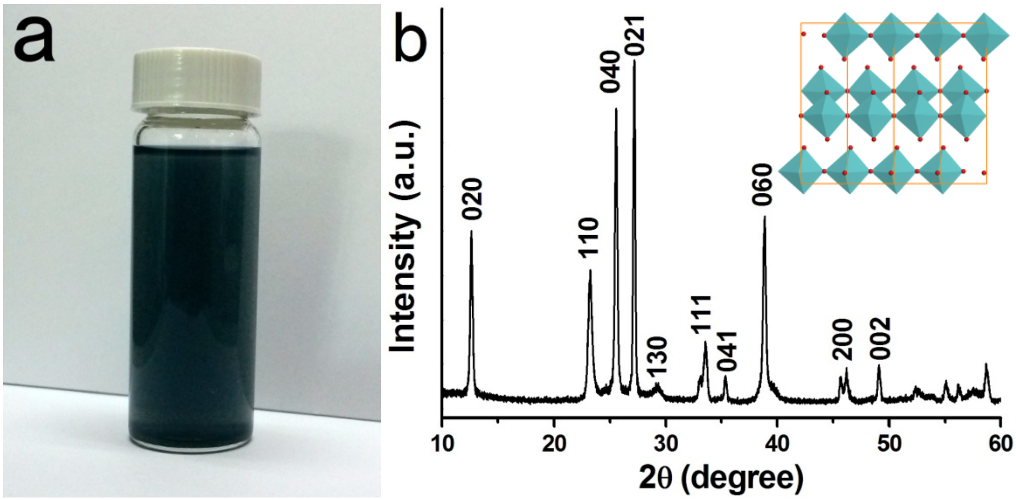

Fig. S1 (a) A photograph of the MoO_{3-x} products dispersed in water. (b) XRD pattern of MoO_{3-x} products, inset: crystal structure.

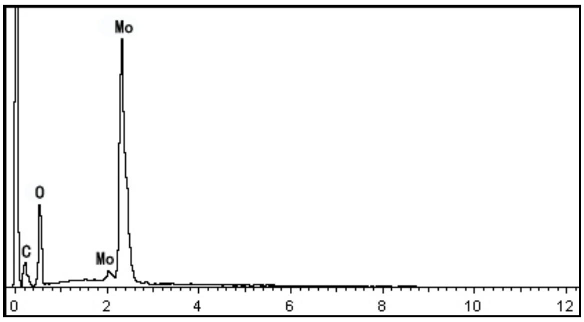

Fig. S2 EDS spectrum of the MoO_{3-x} nanobelts.

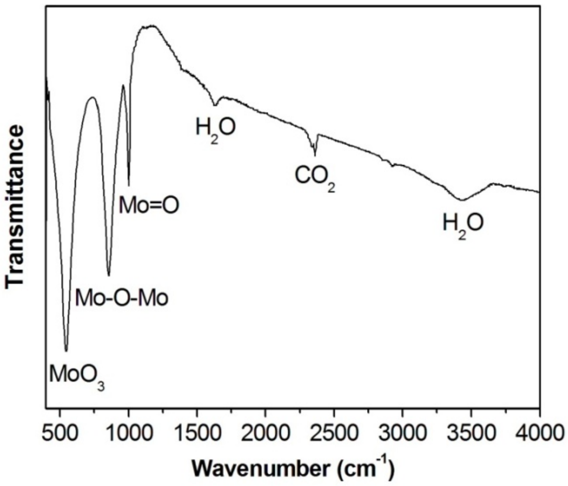

Fig. S3 FTIR spectrum of the as-synthesized MoO_{3-x} nanobelts.

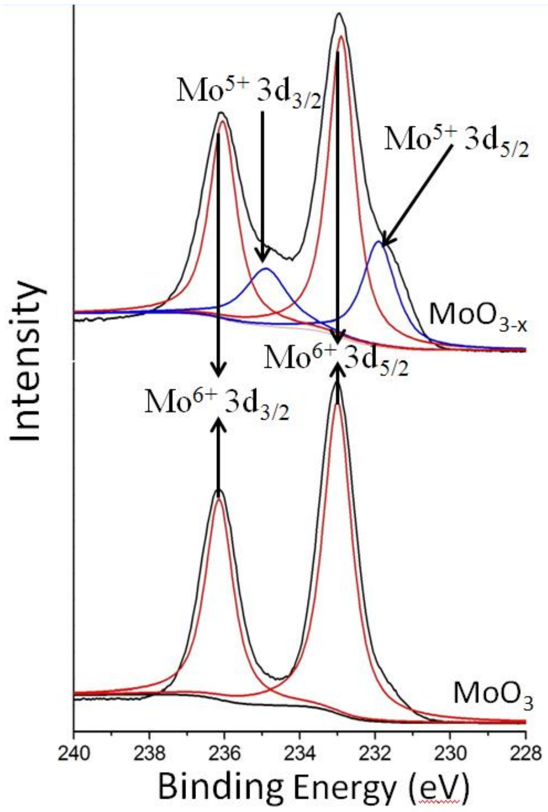

Fig. S4 X-ray photoelectron spectroscopy (XPS) of Mo 3d in the blue MoO_{3-x} nanobelts and commerical MoO_3.

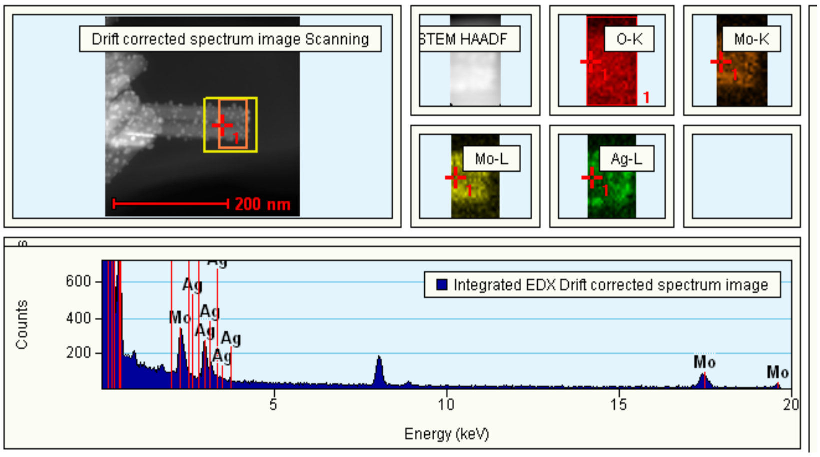

Fig. S5 The EDS mapping results of the Ag/MoO_3 hybrid nanobelts.

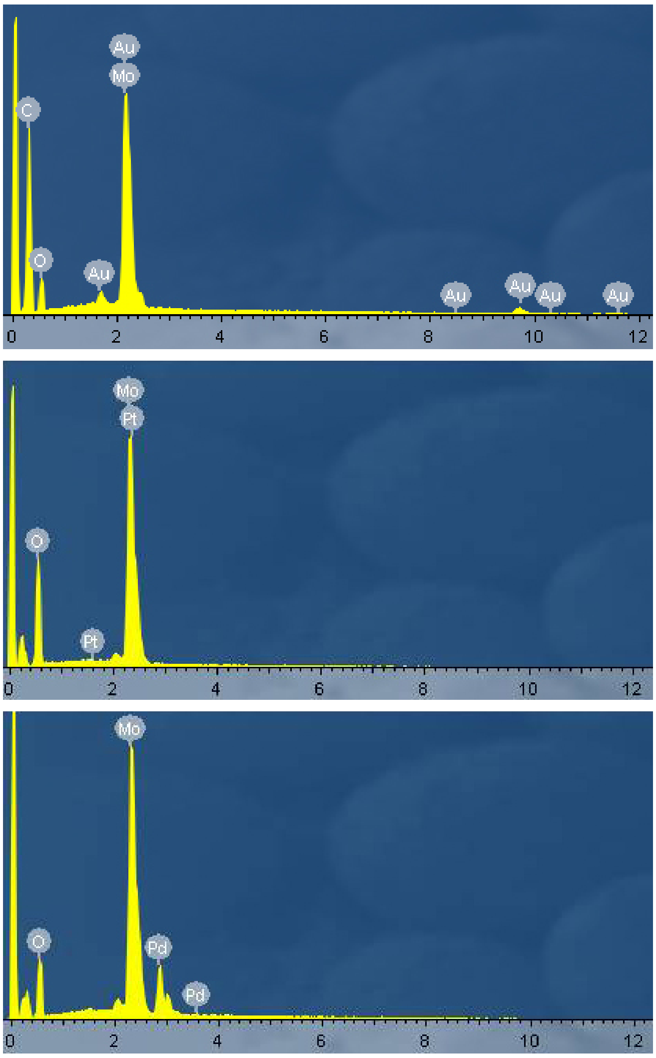

Fig. S6 EDS spectrum of the Au/MoO_3, Pt/MoO_3, and Pd/MoO_3 nanobelts.

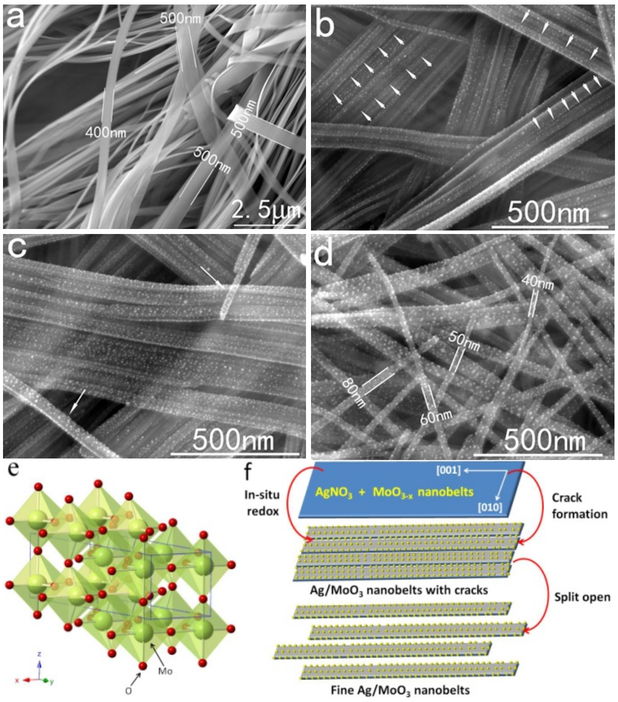

Fig. S7 SEM images of Ag/MoO_3 nanostructures obtained at room temperature after reaction time of (a) 0 h, (b) 6 h, (c) 12 h, and (d) 24 h. (e) Crystal structure of orthorhombic molybdenum oxide. (f) Schematic illustration of the formation and shape evolution of the Ag/MoO_3 nanobelts.

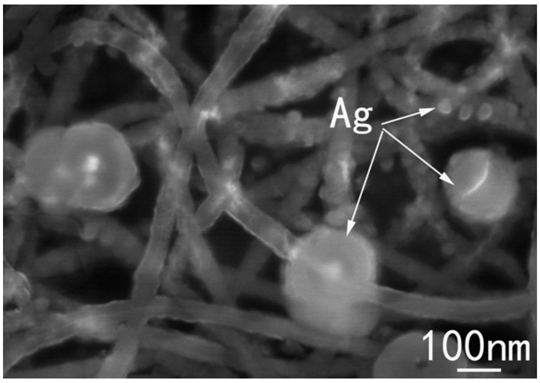

Fig. S8 SEM image of the Ag/MoO_3 nanowires obtained by increasing $AgNO_3$ concentration to 0.02 g/mL.

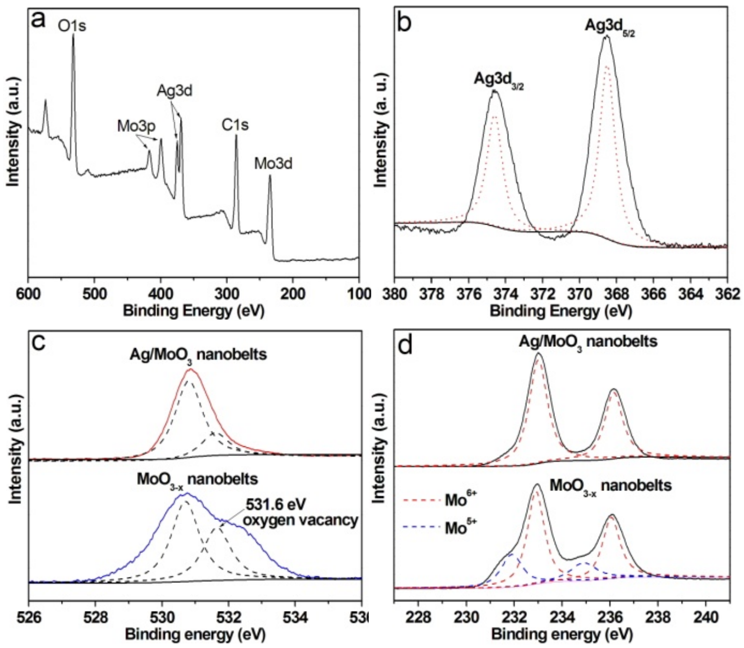

Fig. S9 XPS spectra of the MoO_{3-x} and Ag/MoO_3 nanobelts. (a) Survey spectrum, (b) Ag 3d, (c) O 1s, (d) Mo 3d.

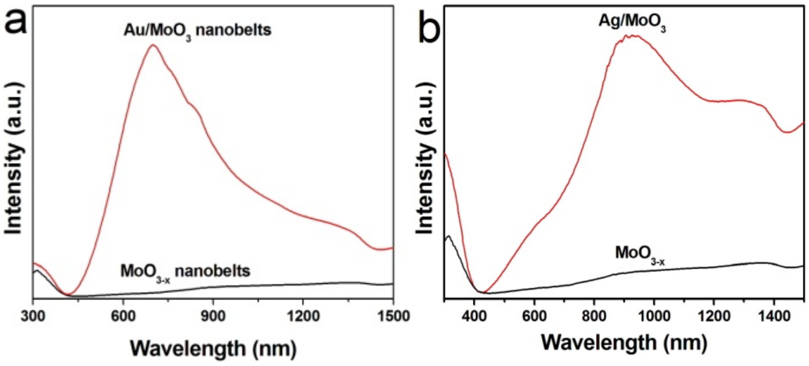

Fig. S10 (a) UV-Vis-NIR adsorption of the as-synthesized Au/MoO$_3$ hybrid nanobelts and MoO$_{3-x}$ nanobelts. **(**b) UV-Vis-NIR adsorption of the as-synthesized Ag/MoO$_3$ hybrid nanobelts and MoO$_{3-x}$ nanobelts.

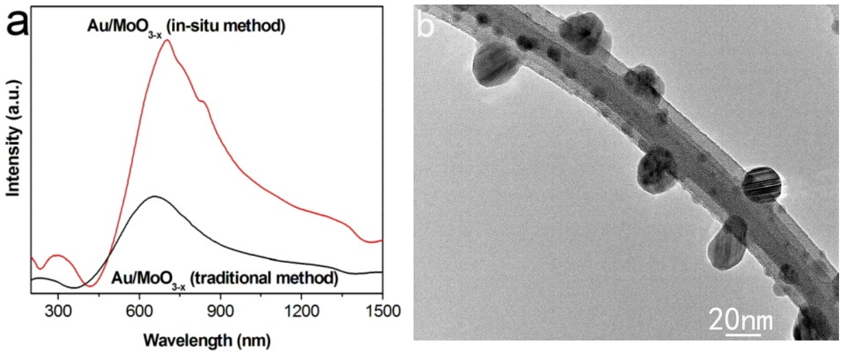

Fig. S11 (a) UV-Vis-NIR absorption spectra of the Au/MoO$_3$ hybrid nanobelts obtained by the present in-situ method and the Au/MoO$_3$ hybrid nanobelts obtained by the traditional loading-high temperature oxidation method. (b) TEM image of the Au/MoO$_3$ obtained the traditional immobilization-high temperature oxidation method. From this image, we can see that the size of the Au nanoparticles becomes very large, from 2-3 nm changes into 20 nm.

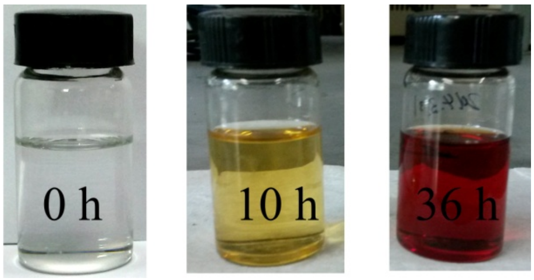

Fig. S12 The photographs of the benzalaniline reaction solution at different reaction steps.

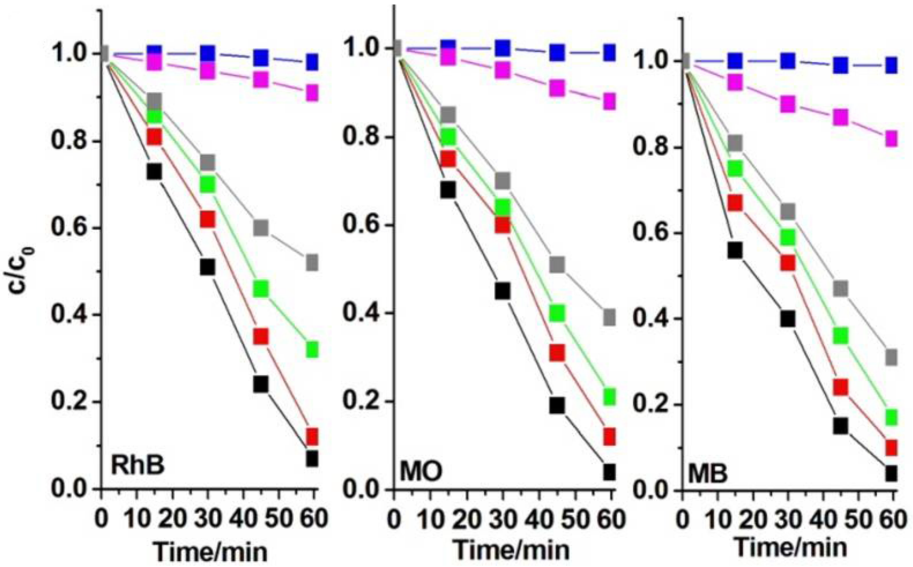

Fig. S13 Photocatalytic activities of six catalysts for the RhB, MO, and MB degradation reactions: Ag/MoO_3 (black), Au/MoO_3 (red), Pt/MoO_3 (green), Au/MoO_3 (gray, prepared by the traditional immobilization-high temperature oxidation method), TiO_2 (P25, magenta), commercial MoO_3 (blue).

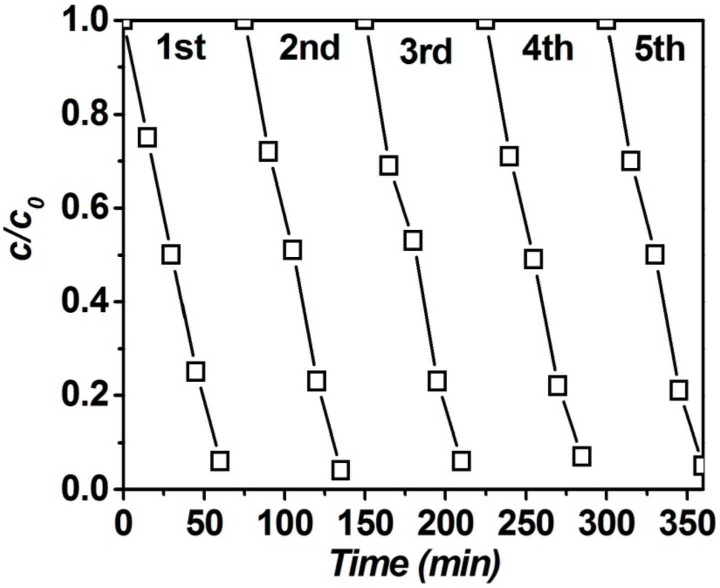

Fig. S14 Recyclability of the photocatalytic decomposition of RhB for the Ag/MoO_3 hybrid nanobelts.

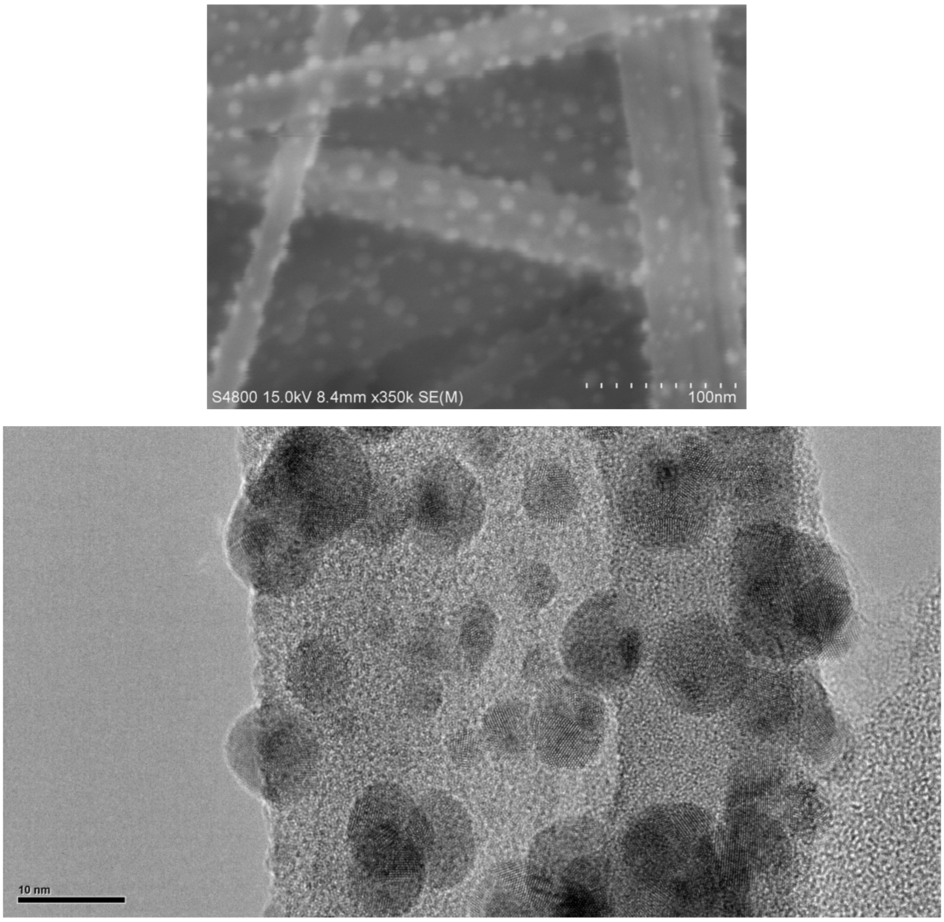

Fig. S15 The SEM and TEM images of the Ag/MoO_3 sample after photocatalytic reaction (5th).